HHS Public Access

Author manuscript

J Pathol. Author manuscript; available in PMC 2016 April 01.

Published in final edited form as:

J Pathol. 2015 April ; 235(5): 731–744. doi:10.1002/path.4484.

BDNF repairs podocyte damage by microRNA-mediated increase of actin polymerization

Min Li[1], **Silvia Armelloni**[1], **Cristina Zennaro**[2], **Changli Wei**[3], **Alessandro Corbelli**[1,4], **Masami Ikehata**[1], **Silvia Berra**[1,5], **Laura Giardino**[1], **Deborah Mattinzoli**[1], **Shojiro Watanabe**[1], **Carlo Agostoni**[6], **Alberto Edefonti**[7], **Jochen Reiser**[3], **Piergiorgio Messa**[8], and **Maria Pia Rastaldi**[1]

[1]Renal Research Laboratory, Fondazione D'Amico per la Ricerca sulle Malattie Renali & Fondazione IRCCS Ca' Granda Ospedale Maggiore Policlinico, Milano, Italy

[2]Laboratory of Renal Physiopathology, Department of Medical, Surgical, and Health Sciences, Trieste University, Trieste, Italy

[3]Department of Medicine, Rush University Medical Center, Chicago, IL, USA

[4]Bio-imaging Unit, Department of Cardiovascular Clinical Pharmacology, Mario Negri Institute of Pharmacological Research, Milano, Italy

[5]"L. Sacco" Department of Biomedical and Clinical Sciences, University of Milano, Italy

[6]Pediatric Clinic 2, Department of Clinical Sciences and Community Health, Clinica Pediatrica De Marchi, Fondazione IRCCS Ca' Granda Ospedale Maggiore Policlinico, University of Milan, Milan, Italy

[7]Division of Pediatric Nephrology and Dialysis, Fondazione IRCCS Ca' Granda Ospedale Maggiore Policlinico, Milano, Italy

[8]Division of Nephrology, Dialysis, and Renal Transplant, Fondazione IRCCS Ca' Granda Ospedale Maggiore Policlinico, Milano, Italy

Abstract

Idiopathic Focal Segmental Glomerulosclerosis (FSGS) is a progressive and proteinuric kidney disease that starts with podocyte injury. Podocytes cover the external side of the glomerular capillary by a complex web of primary and secondary ramifications. Similar to dendritic spines of neuronal cells, podocyte processes rely on a dynamic actin-based cytoskeletal architecture to maintain shape and function. Brain Derived Neurotrophic Factor (BDNF) is a pleiotropic

Corresponding Author: Maria Pia Rastaldi, MD, PhD Renal Research Laboratory Fondazione IRCCS Ca' Granda Ospedale Maggiore Policlinico Via Pace 9 20122 – Milano – Italy Tel +39 0255033879 Fax +39 0255033878 mariapia.rastaldi@policlinico.mi.it.

Conflict of interest statement

Fondazione D'Amico per la Ricerca sulle Malattie Renali is the grantee and Dr Rastaldi is the inventor of US Patent No. 8673851 (issued on March 18, 2014), covering the use of BDNF in proteinuric conditions. Drs. Wei and Reiser have pending or issued patents on the development of novel kidney protective therapies. They stand to gain royalties on their future commercialization.

Author Contributions

Conceived and designed the experiments: RMP, LM, ZC, RJ

Performed the experiments: LM, IM, AS, WC, GL, BS, MD, CA, ZC, WS

Analyzed and discussed the data: RMP, LM, MP, EA, AC, RJ

Wrote the manuscript: RMP, LM, ZC, RJ

neurotrophin that binds to the tropomyosin-related kinase B receptor (TrkB) and has crucial roles in neuron maturation, survival, and activity. In neuronal cultures, exogenously added BDNF increases number and size of dendritic spines. In animal models, BDNF administration is beneficial in both central and peripheral nervous system disorders. Here we show that BDNF has a TrkB-dependent trophic activity on podocyte cell processes; by affecting microRNA-134 and microRNA-132 signaling, BDNF upregulates Limk1 translation and phosphorylation, and increases cofilin phosphorylation which results in actin polymerization. Importantly, BDNF effectively repairs podocyte damage “in vitro”, and contrasts proteinuria and glomerular lesions in “in vivo” models of FSGS, opening a potential new perspective to the treatment of podocyte disorders.

Keywords

Podocyte; Brain Derived Neurotrophic Factor; adriamycin nephropathy; actin cytoskeleton

Introduction

Idiopathic FSGS is a disease of children and adults with unknown origin and clinically characterized by severe protein loss in the urine, causing a further renal demise and increased cardiovascular morbidity and mortality (1). FSGS diagnosis and treatment remain a difficult task for the clinician; even after the introduction of immunomodulators such as Rituximab, a majority of patients do not respond to therapy and progress to end-stage renal failure eventually requiring dialysis or renal transplantation. Furthermore, the frequent relapse of the disease after renal transplant makes dialysis the only option for about 40% of patients. For these reasons, despite being a rare disease, idiopathic FSGS accounts for up to 20% of subjects on dialysis (2). Results from human genetics, transgenic animal models, and functional studies, have been crucial in emphasizing the primary involvement of podocytes in onset and progression of glomerular damage (3).

Podocytes are post-mitotic cells exhibiting a complex array of ramifications consisting of primary major processes that further divide in secondary “foot” processes. Ramifications from a podocyte intertwine with those departing from neighboring cells to form a close net that completely enwraps the glomerular basement membrane. Beginning with morphological clues and supported by a series of molecular discoveries, results from our and other groups have uncovered multiple similarities between podocytes and neuronal cells. Expression studies and functional data have indeed confirmed that podocytes express and utilize molecules previously considered exclusive of the neurons (4-7), and vice versa, several so-called podocyte-specific molecules have been shown relevant to neuronal cells (8-10). The two cell types have a common cytoskeletal organization, with actin mainly concentrated in specialized thin ramifications, i.e. foot processes in podocytes and dendritic spines in neuronal cells, where actin dynamics are critical to shape and function (11, 12).

In neuronal cells, actin remodeling is the driving force of spine formation, shaping, and stabilization. These events are profoundly altered in neurological and psychiatric disorders, such as Alzheimer's disease and schizophrenia, resulting in reduced number and altered

morphology of dendritic spines (13). Similarly, podocyte actin dynamics serve to maintain the regular shape and spacing of foot processes along the glomerular basement membrane; changes become morphologically evident in the loss of the foot process architecture, a manifestation termed foot process effacement. This typical injury pattern is observed in both experimental and human proteinuric conditions and is prominent in glomeruli of FSGS patients (3, 14).

Brain-derived neurotrophic factor (BDNF) is a member of the neurotrophin family of polypeptide growth factors. Neuroprotective effects of exogenous BDNF have been demonstrated in both “in vitro” and “in vivo” models of neuronal cell injury (15-20). Mature BDNF binds to the tropomyosin-related kinase B (TrkB) receptor, which is expressed not only in neuronal cells, but also in several non-neuronal tissues, from embryonic development through adulthood (21). Previous data showed TrkB in developing glomeruli, mature tubules, collecting ducts, and the juxtaglomerular apparatus (21-26). Differences among these reports are most likely due to the use of different techniques, antibodies, and experimental models. As a result, there is still uncertainty about expression and function of TrkB in the kidney. Here we show that mouse and human glomeruli and cultured podocytes indeed express TrkB, which is the target of exogenously administered BDNF. BDNF binding results in reduction of microRNA-134 and increase of microRNA-132, with subsequent effects that ultimately converge to promote actin polymerization and can be exploited to effectively repair podocyte damage “in vitro” and “in vivo”.

Methods

Podocyte cell cultures

Primary podocytes and a podocyte cell line were obtained and maintained as previously described (4). For details, see Online Supporting Information.

Concentration-dependent (10-350ng/ml) and time-dependent (4-72h) studies were performed with Brain Derived Neurotrophic Factor (BDNF, human recombinant, QED Bioscience Inc., Histo Line, Milano, Italy) and Neurotrophic Growth Factor (NGF, human recombinant, Sigma-Aldrich, Milan, Italy), both dissolved in medium. These studies indicated an optimal working concentration of 200 ng/ml for both growth factors, confirming data previously obtained in neuronal cells (27). Results were evaluated at 8, 20, 24, 48, and 72h.

To induce podocyte damage we used protamine sulphate (100μg/ml, 4h), puromycin aminonucleoside (10μg/ml, 24h), and adriamycin (doxorubicin hydrochloride, 0.5μM, 12h) (all from Sigma-Aldrich), dissolved in medium. Thereafter medium was changed and 200ng/ml BDNF or medium alone were added for 24, 48, and 72h.

Osteoblast cell line

The osteoblast MC3T3-E1 line was utilized as negative control for TrkB expression. Details are provided as Online Supporting Information.

Zebrafish model

Zebrafish (wild-type fish, TüAB strain) were kept in a ZEBTEC Bench Top system (Tecniplast, Varese, Italy) and maintained under standard conditions (28). Eggs were protected from predation by the addition of egg traps into tanks prior to spawning.

The newly fertilized eggs were transferred into Petri dishes filled with embryo medium E3 (5mM NaCl, 0.17mM KCl, 0.40mM CaCl2, 0.16mM MgSO4 per 100 ml distilled water). The normally and healthy developed eggs at 6 hours post fertilization (hpf) were then selected under a stereomicroscope (Leica Microsystems GmbH, Wetzlar, Germany) for subsequent applications, and raised at 28°C in E3 medium.

For zebrafish protocols, adriamycin (Sigma-Aldrich) 20μM dissolved in distilled water was added to E3 medium from 9hpf to 57hpf (29), then removed and larvae were divided in two groups of 20 animals each. BDNF 200ng/ml was dissolved in distilled water (vehicle) and added to E3 medium in the first group, whereas the second group received the same quantity of vehicle. Three sets of independent experiments were performed.

A qualitative assay was employed to investigate glomerular blood filtration, as described (30). Briefly, a solution of FITC-labeled 70kDa-dextran (Sigma) was injected into the cardiac venous sinus of 80hpf old early larvae. 30 animals per group and time point were studied. Sequence images of live fish were generated using a Leica inverted microscope connected to a Leica DFC490 camera. Fluorescence intensity of grayscale images of the eye were measured using Sigma Scan Pro software (Jandel Scientific, San Rafael CA, US) and reported in relative units of brightness. Animals with significant amount of FITC-dextran trapped in the yolk sac were excluded from the analysis.

For evaluation of the pericardial edema the cardiac and the total body area were measured off-line by Sigma Scan Pro software, and values expressed as the ratio between cardiac area and total body area.

Mouse adriamycin nephropathy

Adriamycin nephropathy was induced by a single injection of 10mg/Kg doxorubicin hydrochloride in the tail vein of 3 month old male Balb/c mice (Charles River Italia).

Urinary albumin was monitored every other day by Albustix (Bayer, Milan, Italy) and 24h urine collection was performed every 2 to 3 days to measure urinary albumin (Mouse albumin ELISA kit, Bethyl Laboratories, Inc, Montgomery, TX, USA) and urinary creatinine (Urinary creatinine assay kit. Cell Biolabs Inc, San Diego, CA, USA).

From a total of 15 mice initially injected with adriamycin, the 10 reaching 4+ albumin values by Albustix at day 7 were selected and randomized to receive vehicle (5 mice) or BDNF (5 mice) from day 9 to day 13 for a total dosage of 1mg/mouse. Mice were sacrificed on day 16 and the kidneys removed for histology and immunostaining.

An additional group of mice (10 Balb/c animals, male, 3 months of age) was subsequently utilized and the same protocol was applied; after adriamycin injection, 6 animals were selected based on albustix 4+ at day 7 and randomized to receive BDNF (3 mice) or vehicle

(3 mice). Kidneys from this group were utilized for glomerular sieving and western blot studies on glomerular lysates. BDNF dosage, route of administration, and treatment duration were based on published data in models of peripheral nervous system disease (31, 32). A stock solution of 2mg/ml BDNF (QED Bioscience Inc.) in PBS containing 0.1% Tween20 and 1% mannitol was prepared, and 10mg/Kg/die were injected in the tail vein. Control mice received a corresponding amount of PBS plus 0.1% Tween20 and 1% mannitol (vehicle).

In vivo Trkb silencing

Adriamycin nephropathy was induced in 20g male Balb/c mice (8 animals) at day 1 by a single injection of doxorubicin hydrochloride (Sigma-Aldrich) at 10mg/kg body weight. From D9 to D13, BDNF was injected i.v at 10mg/kg/day in 4 mice. The other 4 animals received the same amount of saline instead of BDNF.

SiRNA delivery was achieved with the kidney in vivo transfection reagent (KIDNEY-targeted In Vivo Transfection Reagent, Altogen Biosystems, Las Vegas, US). Vector based TrkB siRNA (NTRK2 - Mouse, 29mer shRNA constructs in retroviral untagged vector, Origene, Rockville, US) was given to 3 mice i.p. at 50μg/mouse 14h before the 1st dose of BDNF and repeated once at day 11. Control mice received the same amount of siRNA scrambles (scrambled negative control siRNA duplex, Origene). Urine was collected before and every 2 to 3 days after doxorubicin injection for urinary albumin and creatinine determination. At day 16, all mice were sacrificed with the kidneys removed for histology and immunostaining.

Double transfection experiments

MicroRNA downregulation was conducted with LNA132, mmu-miR-132 miRCURY LNA™ knockdown probe, 5’fluorescein-labeled (Exiqon) and LNA134, mmu-miR-134 miRCURY LNATM knockdown probe, 5’fluorescein-labeled (Exiqon). Expression plasmids for microRNA overexpression were mouse microRNA134 (Origene) and mouse microRNA132 (kindly provided by Dr Romano Regazzi, University of Lausanne, Switzerland).

DNA was diluted in OptiMEM reduced serum medium together with FuGENE HD Transfection Reagent (Promega), and the transfection mixture added to podocytes.

As controls, we used sense miR159 control, miRCURY LNA™ knockdown probe, 5’fluorescein-labeled, or the transfection mixture without DNA.

Transfection efficiency was evaluated by observing fluorescein expression and resulted in more than 70% efficiency.

In vitro TrkB silencing

Cells were transfected with 200pM siRNA duplexes using Lipofectamine2000 (Invitrogen) as transfection agent. We used a pool of 3 commercially available siRNAs complementary to TrkB mRNA (Sigma-Aldrich). As control, non-targeting siRNAs were applied at the

same concentration. Transfection efficiency was determined by a fluorescent-tagged siRNA (Alexa-Fluor488; Amersham, PerkinElmer, Waltham, MA).

Statistical analyses

Data are presented as mean±SD. At least three replicates were conducted for each in vitro experiment. Two-tail Student's t test was used for analysis of data when two groups of data were compared. ANOVA test was applied when comparing more than 2 groups of data.

For Real-Time RT-PCR data, relative RNA abundance was determined using the comparative Ct method. Fold change error bars represent the standard deviation (σ) of the fold change (FC), according to the following formula: $\sigma = FC*\ln 2*\mathrm{sqrt}(\sigma_x^2/n_x+\sigma_y^2/n_y)$. Pvalues were calculated based on a Student's t-test of the replicate 2^(-DeltaCt) values.

In all statistical analyses, Pvalues <0.05 were considered significant.

Ethical approval

Animal protocols strictly adhered to the Public Health Service Policy on Humane Care and Use of Laboratory Animals (D.L.116-27/01/1992), and were approved by the Milan University Institutional Care and Ethical Treatment Committee and by the Rush University Medical Center Institutional Animal Care and Use Committee.

Online Supporting Methods

Renal tissue processing, immunostaining and evaluation, InCell ELISA, Western Blot, RT-PCR and Real-Time RT-PCR were performed according to standard procedures (details in Online Supporting Information).

Results

TrkB expression in mouse glomeruli and podocytes

Using isoform-specific primers (33), RT-PCR followed by sequencing (Supp. Fig 1-2) showed that mouse glomeruli contain both the full-length and truncated isoform of the BDNF receptor TrkB (Fig 1A). Protein analysis, conducted with an antibody able to recognize full-length TrkB as well as the truncated isoform (34), showed that full-length TrkB prevails in glomerular lysates as well as in brain protein extracts (Fig 1B).

Immunogold electron microscopy detected the receptor mainly in podocytes and to a lesser extent in the glomerular endothelium (Fig 1C). Immunofluorescence concordantly showed TrkB in control mouse glomeruli, where it mostly colocalized with nephrin, supporting a major podocyte expression, and displayed scattered co-staining with the endothelial marker CD31 (Fig 1D).

In human control kidneys, glomerular TrkB was found almost exclusively in podocytes (Supp. Fig 3). Differently from mice, the molecule was observed in proximal tubuli. Expression of TrkB was maintained by cultured murine cells, both primary podocytes and the cell line (4), as proven by RTPCR, WB, and immunostaining (Supp. Fig 4).

BDNF increases number and length of podocyte processes

In vitro, 200ng/ml BDNF increased both number and length of podocyte processes, particularly in primary podocytes (Supp. Fig 5). Changes became morphologically evident after 20 hours incubation and were attributable to increased F-actin, as shown by phalloidin staining (Fig 2A, Supp. Fig 6A).

Despite nephrin was more evident along podocyte processes (Fig 2A), its expression was not increased (Supp. Fig 6A). BDNF incubation resulted in upregulation of TrkB expression (from 5.4±0,2 to 9.2±0.2nm, by inCell-ELISA) (Fig 2A, Supp. Fig 6A-B) and phosphorylation (from 4.3±0.8 to 6.7±0.3nm) (Supp. Fig 6A).

BDNF effects were abolished by TrkB silencing (Fig 2A, Supp. Fig 6B), indicating that exogenous BDNF acts on podocytes in a TrkB-dependent manner. Addition of NGF, whose receptor TrkA was shown in glomeruli (25-26, 35), did not produce similar effects (Supp. Fig 7).

BDNF effects are mediated by microRNA-134 and microRNA-132

The observed sprouting and elongation of podocyte cell processes with F-actin upregulation entail increased actin polymerization; indeed, increased cofilin phosphorylation was observed after 24h BDNF exposure (Supp. Fig 8A). Phosphorylation of cofilin is mostly due to the kinase Limk1 (36). Therefore, not surprisingly, we observed that BDNF treatment led to Limk1 overexpression and phosphorylation, both abolished by TrkB silencing (Fig 2B, Supp. Fig 8B). Increased Limk1 protein was not sustained by increased transcription, because Limk1 mRNA did not show any changes after BDNF exposure (Supp. Fig 8C). Therefore, we hypothesized the intervention of post-transcriptional mechanisms, such as those regulated by microRNAs (miRNAs). Limk1 mRNA is a direct target of miRNA134 (37). Furthermore, miRNA132 was shown to indirectly increase Limk1 translation, by targeting the mRNA of p250GAP, a molecule that blocks Rac1 activity (38).

Both miRNA134 and miRNA132 (Supp. Fig 9A) were found in mouse glomeruli and podocytes. Similarly to neuronal cells (39), podocytes seem to express little endogenous miRNA134 and contain higher levels of miRNA132 in control conditions. BDNF time-dependently further downregulated miRNA134 and upregulated miRNA132 (Supp. Fig 9B, 9C). While a decrease of miRNA134 directly augments Limk1 translation, the rise of miRNA132 would obtain indirectly the same effect by reducing p250GAP translation (38-40), therefore relieving the blockade of Rac1, which in turn increases Limk1. Confirming this pathway, we observed a reduction of p250GAP protein expression in BDNF-incubated podocytes (Supp. Fig 10A, 10B), and supporting the post-transcriptional nature of this event, p250GAP protein changes were not paralleled by a decrement of the mRNA (Supp. Fig 10C). Taken together, these data show that podocytes indeed express miRNA134 and 132, which are differentially regulated by exogenous BDNF, ultimately increasing Limk1 translation and phosphorylation, which affect cofilin activity and favor actin polymerization.

To further prove these miRNA-mediated events, we mimicked BDNF action by overexpressing miRNA132 and silencing miRNA134 in cultured podocytes. After 48h from

double transfection, we observed a pronounced elongation of cell processes (Fig 3A, 3B), accompanied by increased phosphorylation of cofilin and reduced expression of p250GAP (Fig 3C). On the contrary, miRNA134 overexpression coupled to silencing of miRNA132 caused cell rounding with evident shortening of cell processes (Fig 3A, 3B); accordingly, phospho-cofilin was profoundly reduced and p250GAP did not change as compared to control cells (Fig 3C).

BDNF repairs podocyte damage in vitro

Next, we tested if BDNF could treat podocyte injury caused by substances which are commonly used to reproduce nephrotic podocyte changes “in vitro”, such as protamine sulfate, puromycin aminonucleoside, and adriamycin. Similar results were obtained with all three compounds. After removal of the drug, podocytes incubated with 48h medium alone displayed shortened cell processes and large remodeling of the actin and myosin cytoskeleton, with loss of filament bundles and rounding of the cell shape (Supp. Fig 11A, 12). Medium supplementation with BDNF determined complete repair of podocyte morphology, with full recovery of the actin-myosin cytoskeleton (Supp. Fig 11A, 12). Quantification of immunostaining by InCell ELISA showed that BDNF was able to restore expression of TrkB, pTrkB, nephrin, Limk1, p-Limk1, cofilin, p-cofilin, and myosin2A, and to reduce p250GAP (Supp. Fig 11B). TrkB silencing abolished BDNF action, as shown by persisting morphological changes and reduction of phosphorylated cofilin (Supp. Fig 13).

In vivo effects of BDNF administration

Based on what obtained “in vitro”, we moved to “in vivo” conditions. Animal experiments were first conducted on Zebrafish larvae in which 20μM Adr was added to the medium as early as 9 hours post-fertilization (hpf) (Supp. Fig 14A). After 48h incubation, Adr invariably caused pericardial edema (Supp. Fig 14B), which further increased at 5 days post-fertilization (dpf) in vehicle-treated larvae (Supp. Fig 14C). Electron microscopy showed a profound impairment of podocyte process development (Fig 4A). Reduction of nephrin and TrkB was documented by Real Time RT-PCR (Fig 4B). BDNF treatment significantly reduced the cardiac/body ratio, completely normalized podocyte process formation, and restored expression of nephrin and TrkB1 to the levels observed in control larvae (Fig 4A, 4B).

Microinjection of 70-kDa FITC-labeled dextran in control animals resulted in homogeneous fluorescence distribution in the cell body, that remained stable up to 24h, then declined at 48h (Fig 4C). Larvae exposed to adriamycin had globally decreased fluorescence, due to accelerated dextran clearance through the damaged glomerulus. Measurement of eye fluorescence showed rapid and dose-dependent decline in fish exposed to adriamycin (Fig 4C). Supporting morphological and expression studies, dextran clearance was similar to control values after BDNF treatment (Fig 4D).

In mouse adriamycin nephropathy, we observed progressive increase of albuminuria (Supp. Fig 15A). The histological exam of the kidneys displayed focal and segmental glomerular damage and evident tubular protein casts (Fig 5A, Supp. Fig 15B). Extensive effacement of podocyte foot processes was observed by transmission and scanning electron microscopy

(Fig 5B). BDNF treatment profoundly reduced albuminuria, which at sacrifice was almost back to control values (Supp. Fig 15A) and significantly ameliorated glomerular damage (Fig 5A, Supp. Fig 15B). Dilated tubules, though devoid of protein casts, were still found in the interstitium of BDNF-treated animals. Transmission and scanning electron microscopy highlighted the wide recovery of podocyte foot processes (Fig 5B).

In addition, BDNF treatment increased glomerular nephrin, TrkB, p-cofilin, F-actin, and p-Limk1, as demonstrated by immunofluorescence and western blot (Supp. Fig 15C, 16, 17). To further assess the specificity of BDNF treatment, glomerular TrkB silencing was obtained by administering a vector-based TrkB siRNA after adriamycin injection (Supp. Fig 18A). This largely reduced the anti-proteinuric effect of BDNF, which was instead preserved after injection of a scramble-siRNA (Supp. Fig 18B). Concordantly, histology and immunofluorescence showed that efficacy of BDNF in treating glomerular damage was severely blunted by TrkB silencing (Fig 6, Supp. Fig 19, 20).

Discussion

Our results show a trophic activity of exogenous BDNF on the cytoskeleton of podocyte cell processes, that can be utilized to repair podocyte damage “in vitro” and “in vivo”. Most experimental data on BDNF administration have been obtained on neuronal and glial cells, in which the neurotrophin is known to bind and activate the tropomyosin-related kinase B receptor (TrkB), also known as Neurotrophin Tyrosine Kinase Receptor 2 (Ntrk2) (41).

Besides the nervous system, TrkB expression has been demonstrated in a variety of cells and organs, making them sensitive to the action of BDNF administration. For instance, BDNF application on TrkB-expressing brain endothelial cells resulted in improved cell survival and angiogenesis (42). Similarly, exogenous BDNF was shown to induce differentiation and protect TrkB-expressing cementoblasts from cell death (43).

Binding of mature BDNF to TrkB causes receptor dimerization and autophosphorylation, with consequent activation of multiple pro-survival signaling pathways (41). Additional BDNF-dependent signaling is due to the existence of truncated isoforms of the receptor, which can form heterodimers with the full-length isoform and mostly behave as a dominant negative molecule or can signal independently as a monomer (44). Due to the prevailing presence of TrkB in glomerular podocytes, we focused our attention on these cells. Interestingly, BDNF exposure in vitro caused striking morphological changes in terms of length and number of podocyte ramifications.

Similar changes have been repeatedly observed in neuronal cells, in which BDNF application increased axon length and significantly augmented the number of dendritic spines and synaptic contacts (45-47). Dendritic spines and podocyte processes rely on a common cytoskeletal organization, based on actin as the main cytoskeletal protein and the final target of multiple physiological as well as pathological signaling pathways (48, 49, 11).

The importance of actin in podocyte biology and disease is well established. As the main cytoskeletal component of podocyte processes, actin is the molecule ultimately responsible for podocyte shape and function. The changes commonly observed in podocyte damage, i.e.

loss of stress fibers, cell rounding and shortening of ramifications “in vitro”, and foot process effacement and microvillous transformation “in vivo”, are determined by alterations of actin dynamics (11).

Actin filament dynamics and reorganization are spatiotemporally regulated by numerous actin-binding proteins and upstream signaling molecules, which cooperatively control assembly and disassembly of actin filaments (50). Among these proteins, the actin-depolymerizing factor (ADF)/cofilin family proteins stimulate depolymerization of actin filaments, playing a crucial role in actin dynamics and reorganization of actin filaments (51). The presence and relevance of cofilin-1 in podocyte foot process homeostasis have been demonstrated by Garg et al. (52). Cofilin-1 is inactivated by phosphorylation, which is mostly regulated by the kinase Limk1 (36). Not surprisingly, BDNF incubation in podocytes resulted in increased cofilin phosphorylation and increased content of Limk1 and phospho-Limk1.

Regulation of Limk1 has been widely studied in the context of synaptic spine growth and plasticity, which need tight regulation during neuronal development as well as in mature neuronal cells. Limk-1-KO mice exhibit significant abnormalities in spine morphology and synaptic function (53). In humans, loss of Limk-1 appears implicated in a mental disorder with profound deficits in visuo-spatial cognition (54) and a polymorphism of Limk-1 promoter has been associated with decreased Limk-1 mRNA and formation of intracranial aneurysms (55). In dendritic spines, Limk1 is kept under direct control by miRNA-134. Furthermore, miRNA-132 has been found to regulate Limk1 by reducing the expression levels of p250GAP (37-40).

Our results show the involvement of both these miRNAs in BDNF regulation of podocyte processes, further extending the similarities between dendritic spine and podocyte process dynamics. In healthy podocytes the cytoskeletal changes caused by BDNF are not good “per se”, because they alter a highly regulated equilibrium in favor of actin polymerization. Instead, these same effects are beneficial when occurring after podocyte damage, because BDNF seems to favor a much needed podocyte process elongation that contrasts the flattening induced in nephrotic conditions both “in vitro” and “in vivo”. Indeed, because of the action on actin polymerization, BDNF seems to target the final common pathway on which different types of damaging events ultimately merge and could be useful in the treatment of podocyte damage in several proteinuric conditions, especially FSGS.

Given the actin-trophic effects, BDNF has been considered as a candidate powerful drug in several neurological diseases. Encouraging results have been obtained in several experimental models of neurological diseases (17-19), but human trials have failed so far, mainly because of the difficulty of BDNF to cross the blood brain barrier (41). Remarkably, during the largest and longest trial conducted on 748 subjects affected by Amyotrophic Lateral Sclerosis (56) who were injected daily with BDNF for 9 months, no patients experienced neuropathic pain and only minor side effects were reported, supporting its safety in humans. However, TrkB is also expressed by several types of neuronal, epithelial and connective tumor cells (57). Thus, a podocyte-targeted BDNF delivery is likely to be needed to increase efficacy and specificity and avoid side-effects. Nevertheless, the idea to

target a common downstream pathway, i.e. actin in podocytes, may harbor a novel approach to combat podocyte injury in proteinuric diseases.

Supplementary Material

Refer to Web version on PubMed Central for supplementary material.

Acknowledgments

The work was supported by grants from Fondazione La Nuova Speranza Lotta alla Glomerulosclerosi Focale and Associazione Bambino Nefropatico ABN ONLUS to the Renal Research Laboratory, and by grants from the National Institutes of Health (DK073495 and DK089394) to RJ. During the experiments, ZC was the recipient of a EMBO/ERA-EDTA long term fellowship. The authors deeply thank Guido Brusini for expert technical support, Dr Romano Regazzi for providing the miRNA132 plasmid, and Dr T. Yamamoto and T. Nakazawa for the p250GAP antibody.

References

1. Gbadegesin R, Lavin P, Foreman J, et al. Pathogenesis and therapy of focal segmental glomerulosclerosis: an update. Pediatr Nephrol. 2011; 26(7):1001–1015. [PubMed: 21110043]
2. Braun N, Schmutzler F, Lange C, et al. Immunosuppressive treatment for focal segmental glomerulosclerosis in adults. Cochrane Database Syst Rev. 2008; (3):CD003233. [PubMed: 18646090]
3. Reiser J, Sever S. Podocyte biology and pathogenesis of kidney disease. Annu Rev Med. 2013; 64:357–366. [PubMed: 23190150]
4. Giardino L, Armelloni S, Corbelli A, et al. Podocyte glutamatergic signaling contributes to the function of the glomerular filtration barrier. J Am Soc Nephrol. 2009; 20(9):1929–1940. [PubMed: 19578006]
5. Puliti A, Rossi PI, Caridi G, et al. Albuminuria and glomerular damage in mice lacking the metabotropic glutamate receptor 1. Am J Pathol. 2011; 178(3):1257–1269. [PubMed: 21356376]
6. Brunskill EW, Georgas K, Rumballe B, et al. Defining the molecular character of the developing and adult kidney podocyte. PLoS One. 2011; 6(9):e24640. [PubMed: 21931791]
7. Boerries M, Grahammer F, Eiselein S, et al. Molecular fingerprinting of the podocyte reveals novel gene and protein regulatory networks. Kidney Int. 2013; 83(6):1052–1064. [PubMed: 23364521]
8. Vitureira N, Andrés R, Pérez-Martínez E, et al. Podocalyxin is a novel polysialylated neural adhesion protein with multiple roles in neural development and synapse formation. PLoS One. 2010; 5(8):e12003. [PubMed: 20706633]
9. Li M, Armelloni S, Ikehata M, et al. Nephrin expression in adult rodent central nervous system and its interaction with glutamate receptors. J Pathol. 2011; 225(1):118–128. [PubMed: 21630272]
10. Armelloni S, Li M, Messa P, et al. Podocytes: a new player for glutamate signaling. Int J Biochem Cell Biol. 2012; 44(12):2272–2277. [PubMed: 23018105]
11. Faul C, Asanuma K, Yanagida-Asanuma E, et al. Actin up: regulation of podocyte structure and function by components of the actin cytoskeleton. Trends Cell Biol. 2007; 17(9):428–437. [PubMed: 17804239]
12. Cingolani LA, Goda Y. Actin in action: the interplay between the actin cytoskeleton and synaptic efficacy. Nat Rev Neurosci. 2008; 9(5):344–356. [PubMed: 18425089]
13. Sala C, Segal M. Dendritic spines: the locus of structural and functional plasticity. Physiol Rev. 2014; 94(1):141–188. [PubMed: 24382885]
14. Greka A, Mundel P. Cell biology and pathology of podocytes. Annu Rev Physiol. 2012; 74:299–323. [PubMed: 22054238]
15. Morse JK, Wiegand SJ, Anderson K, et al. Brain-derived neurotrophic factor (BDNF) prevents the degeneration of medial septal cholinergic neurons following fimbria transection. J Neurosci. 1993; 13(10):4146–4156. [PubMed: 8080477]

16. Yurek DM, Lu W, Hipkens S, et al. BDNF enhances the functional reinnervation of the striatum by grafted fetal dopamine neurons. Exp Neurol. 1996; 137(1):105–118. [PubMed: 8566202]
17. Han BH, Holtzman DM. BDNF protects the neonatal brain from hypoxic-ischemic injury in vivo via the ERK pathway. J Neurosci. 2000; 20(15):5775–5781. [PubMed: 10908618]
18. Arancibia S, Silhol M, Moulière F, et al. Protective effect of BDNF against beta-amyloid induced neurotoxicity in vitro and in vivo in rats. Neurobiol Dis. 2008; 31(3):316–326. [PubMed: 18585459]
19. Nagahara AH, Merrill DA, Coppola G, et al. Neuroprotective effects of brain-derived neurotrophic factor in rodent and primate models of Alzheimer's disease. Nat Med. 2009; 15(3):331–337. [PubMed: 19198615]
20. Stahl K, Mylonakou MN, Skare Ø, et al. Cytoprotective effects of growth factors: BDNF more potent than GDNF in an organotypic culture model of Parkinson's disease. Brain Res. 2011; 1378:105–118. [PubMed: 21236244]
21. Yamamoto M, Sobue G, Yamamoto K, et al. Expression of mRNAs for neurotrophic factors (NGF, BDNF, NT-3, and GDNF) and their receptors (p75NGFR, trkA, trkB, and trkC) in the adult human peripheral nervous system and nonneural tissues. Neurochem Res. 1996; 21(8):929–938. [PubMed: 8895847]
22. García-Suárez O, González-Martínez T, Germana A, et al. Expression of TrkB in the murine kidney. Microsc Res Tech. 2006; 69(12):1014–1020. [PubMed: 17013912]
23. De Girolamo P, Arcamone N, Lucini C, et al. TRK neurotrophin receptor-like proteins in the kidney of frog (Rana esculenta) and lizard (Podarcis sicula): an immunohistochemical study. Anat Embryol (Berl). 2004; 207(6):481–487. [PubMed: 14758546]
24. De Girolamo P, Arcamone N, Lucini C, et al. The teleost kidney expresses Trk neurotrophin receptor-like proteins. Anat Embryol (Berl). 2000; 201(5):429–433. [PubMed: 10839637]
25. Shibayama E, Koizumi H. Cellular localization of the Trk neurotrophin receptor family in human non-neuronal tissues. Am J Pathol. 1996; 148(6):1807–1818. [PubMed: 8669468]
26. Durbeej M, Söderström S, Ebendal T, et al. Differential expression of neurotrophin receptors during renal development. Development. 1993; 119(4):977–989. [PubMed: 8306895]
27. Jin X, Hu H, Mathers PH, et al. Brain-Derived Neurotrophic Factor Mediates Activity-Dependent Dendritic Growth in Nonpyramidal Neocortical Interneurons in Developing Organotypic Cultures. J. Neurosci. 2003; 23(13):5662–5673. [PubMed: 12843269]
28. Westerfield, M. A guide for the laboratory use of zebrafish (Danio rerio). 4th ed.. Univ. of Oregon Press; Eugene: 2000. The zebrafish book..
29. Zennaro C, Mariotti M, Carraro M, et al. Podocyte Developmental Defects Caused by Adriamycin in Zebrafish Embryos and Larvae: A Novel Model of Glomerular Damage. PLoS ONE. 2014; 9(5):e98131. doi:10.1371/journal.pone.0098131. [PubMed: 24845233]
30. Hentschel DM, Mengel M, Boehme L, et al. Rapid screening of glomerular slit diaphragm integrity in larval zebrafish. Am J Physiol Renal Physiol. 2007; 293(5):F1746–F1750. [PubMed: 17699558]
31. Yan Q, Matheson C, Lopez OT, et al. The biological responses of axotomized adult motoneurons to brain-derived neurotrophic factor. J Neurosci. 1994; 14(9):5281–5291. [PubMed: 8083736]
32. Schäbitz WR, Steigleder T, Cooper-Kuhn CM, et al. Intravenous brain-derived neurotrophic factor enhances poststroke sensorimotor recovery and stimulates neurogenesis. Stroke. 2007; 38(7): 2165–2172. [PubMed: 17510456]
33. Ninkina N, Adu J, Fischer A, et al. Expression and function of TrkB variants in developing sensory neurons. EMBO J. 1996; 15(23):6385–6393. [PubMed: 8978665]
34. Cazorla M, Arrang JM, Prémont J. Pharmacological characterization of six trkB antibodies reveals a novel class of functional agents for the study of the BDNF receptor. Br J Pharmacol. 2011; 162(4):947–960. [PubMed: 21039416]
35. Bonofiglio R, Antonucci MT, Papalia T, et al. Nerve growth factor (NGF) and NGF-receptor expression in diseased human kidneys. J Nephrol. 2007; 20(2):186–195. [PubMed: 17514623]
36. Scott RW, Olson MF. LIM kinases: function, regulation and association with human disease. J Mol Med (Berl). 2007; 85(6):555–568. [PubMed: 17294230]
37. Schratt GM, Tuebing F, Nigh EA, et al. A brain-specific microRNA regulates dendritic spine development. Nature. 2006; 439(7074):283–289. [PubMed: 16421561]

38. Wayman GA, Davare M, Ando H, et al. An activity-regulated microRNA controls dendritic plasticity by down-regulating p250GAP. Proc Natl Acad Sci U S A. 2008; 105(26):9093–9098. [PubMed: 18577589]
39. Numakawa T, Richards M, Adachi N, et al. MicroRNAfunction and neurotrophin BDNF. Neurochem Int. 2011; 59(5):551–558. [PubMed: 21723895]
40. Marler KJ, Suetterlin P, Dopplapudi A, et al. BDNF promotes axon branching of retinal ganglion cells via miRNA-132 and p250GAP. J Neurosci. 2014; 34(3):969–979. [PubMed: 24431455]
41. Lu B, Nagappan G, Guan X, et al. BDNF-based synaptic repair as a disease-modifying strategy for neurodegenerative diseases. Nat Rev Neurosci. 2013; 14(6):401–416. [PubMed: 23674053]
42. Kim H, Li Q, Hempstead BL, et al. Paracrine and autocrine functions of brain-derived neurotrophic factor (BDNF) and nerve growth factor (NGF) in brain-derived endothelial cells. J Biol Chem. 2004; 279(32):33538–33546. [PubMed: 15169782]
43. Kajiya M, Shiba H, Fujita T, et al. Brain-derived neurotrophic factor protects cementoblasts from serum starvation-induced cell death. J Cell Physiol. 2009; 221(3):696–706. [PubMed: 19711359]
44. Fenner BM. Truncated TrkB: beyond a dominant negative receptor. Cytokine Growth Factor Rev. 2012; 23(1-2):15–24. [PubMed: 22341689]
45. Tyler WJ, Pozzo-Miller LD. BDNF enhances quantal neurotransmitter release and increases the number of docked vesicles at the active zones of hippocampal excitatory synapses. J Neurosci. 2001; 21(12):4249–4258. [PubMed: 11404410]
46. Tyler WJ, Pozzo-Miller L. Miniature synaptic transmission and BDNF modulate dendritic spine growth and form in rat CA1 neurones. J Physiol. 2003; 553(Pt2):497–509. [PubMed: 14500767]
47. Ji Y, Pang PT, Feng L, et al. Cyclic AMP controls BDNF-induced TrkB phosphorylation and dendritic spine formation in mature hippocampal neurons. Nat Neurosci. 2005; 8(2):164–172. [PubMed: 15665879]
48. Hotulainen P, Hoogenraad CC. Actin in dendritic spines: connecting dynamics to function. J Cell Biol. 2010; 189(4):619–629. [PubMed: 20457765]
49. Segal M, Vlachos A, Korkotian E. The spine apparatus, synaptopodin, and dendritic spine plasticity. Neuroscientist. 2010; 16(2):125–31. [PubMed: 20400711]
50. Theriot JA. Regulation of the actin cytoskeleton in living cells. Semin Cell Biol. 1994; 5(3):193–199. [PubMed: 7919233]
51. Mizuno K. Signaling mechanisms and functional roles of cofilin phosphorylation and dephosphorylation. Cell Signal. 2013; 25(2):457–469. [PubMed: 23153585]
52. Garg P, Verma R, Cook L, et al. Actin-depolymerizing factor cofilin-1 is necessary in maintaining mature podocyte architecture. J Biol Chem. 2010; 285(29):22676–22688. [PubMed: 20472933]
53. Meng Y, Zhang Y, Tregoubov V, et al. Abnormal spine morphology and enhanced LTP in LIMK-1 knockout mice. Neuron. 2002; 35(1):121–133. [PubMed: 12123613]
54. Gray V, Karmiloff-Smith A, Funnell E, et al. In-depth analysis of spatial cognition in Williams syndrome: A critical assessment of the role of the LIMK1 gene. Neuropsychologia. 2006; 44(5): 679–685. [PubMed: 16216290]
55. Akagawa H, Tajima A, Sakamoto Y, et al. A haplotype spanning two genes, ELN and LIMK1, decreases their transcripts and confers susceptibility to intracranial aneurysms. Hum Mol Genet. 2006; 15(10):1722–1734. [PubMed: 16611674]
56. A controlled trial of recombinant methionyl human BDNF in ALS: The BDNF Study Group (Phase III). Neurology. 1999; 52(7):1427–1433. [PubMed: 10227630]
57. Thiele CJ, Li Z, McKee AE. On Trk--the TrkB signal transduction pathway is an increasingly important target in cancer biology. Clin Cancer Res. 2009; 15(19):5962–5967. [PubMed: 19755385]

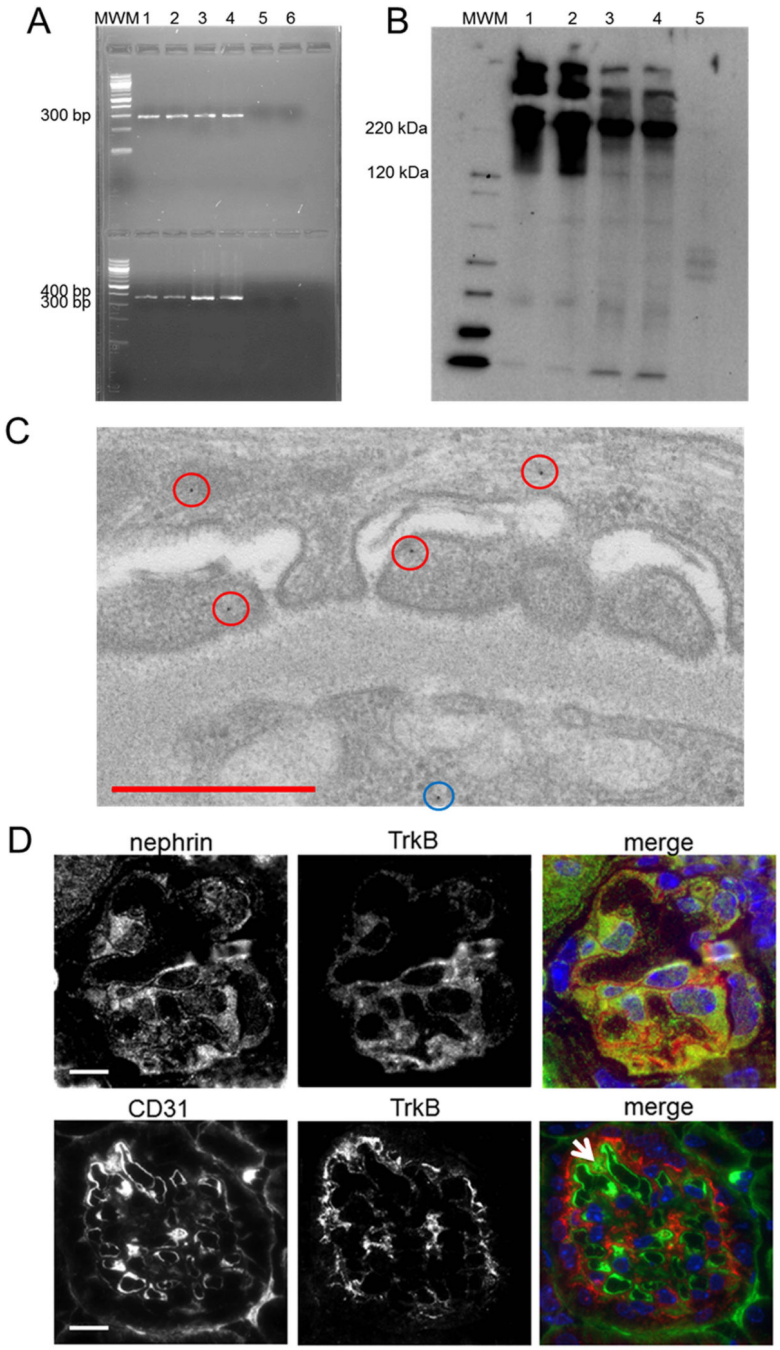

Fig 1. TrkB expression in renal tissue and cultured podocytes

A) RT-PCR results show presence of the full-length (281 bp) and truncated (353 bp) TrkB isoforms in preparations from brain (lane 1), cerebellum (lane 2), and isolated mouse glomeruli (lane 3 and 4). MWM: molecular weight marker; lane 5: negative control, i.e. PCR products obtained from the osteoblast cell line MC3T3-E1; lane 7: PCR negative control.

B) Western Blot (WB) analysis was conducted on protein extracts from mouse brain (1), cerebellum (2) and two preparations of isolated glomeruli (3, 4) in non-reducing conditions.

A band slightly higher than 120kDa, corresponding to the full length molecule, is present in all lanes. In addition, higher bands are observable. Bands of lower molecular weight can be detected as well. MWM = molecular weight marker, Lane 5 = negative control, performed by loading protein lysates from the osteoblast cell line.

C) Immunogold, conducted on a cryosection from control mouse kidney, shows TrkB positivity in a podocyte (red circles) and a dot in an endothelial cell (light blue circle). Scale bar 500nm.

D) Double staining shows that TrkB mostly co-localizes with nephrin (upper panels) and seldom with CD31 (lower panels, arrow). Scale bars 10μm.

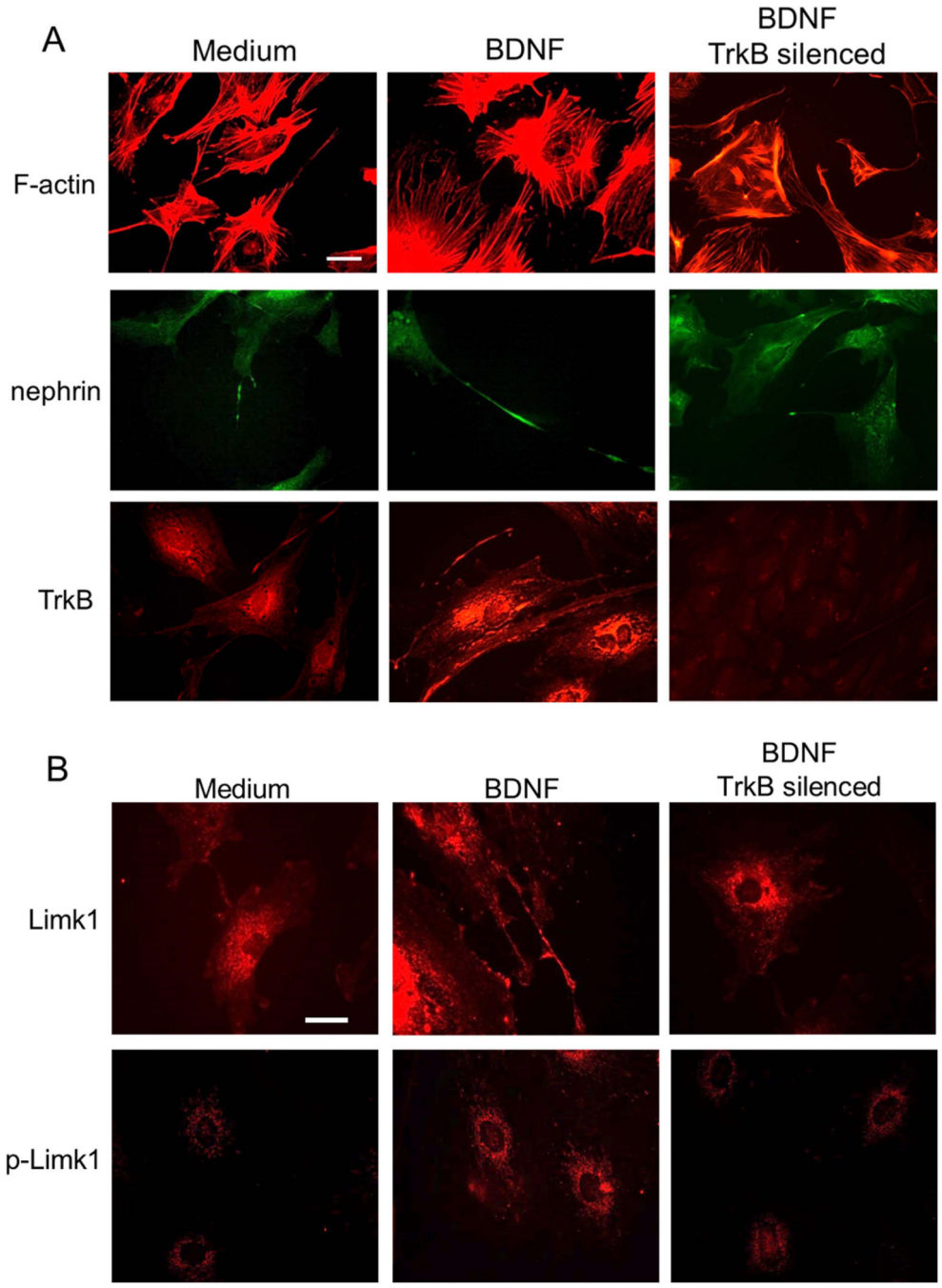

Fig 2. BDNF effects on podocyte processes

A) Immunostaining highlights the effects of BDNF (middle column) as compared to control medium (left column). Phalloidin staining of filamentous actin (F-actin) emphasizes stress fibers and cell ramifications, which appear more developed after BDNF incubation. Nephrin positivity is evident along elongated cell processes, and TrkB expression looks increased. All changes are abolished by TrkB silencing (right column). Scale bar 20μm.

B) Limk1 and pLimk1 show increased expression after BDNF treatment (middle panels) as compared to control (left panels). BDNF effects are abolished by TrkB silencing (right panels). Scale bar 30 μm.

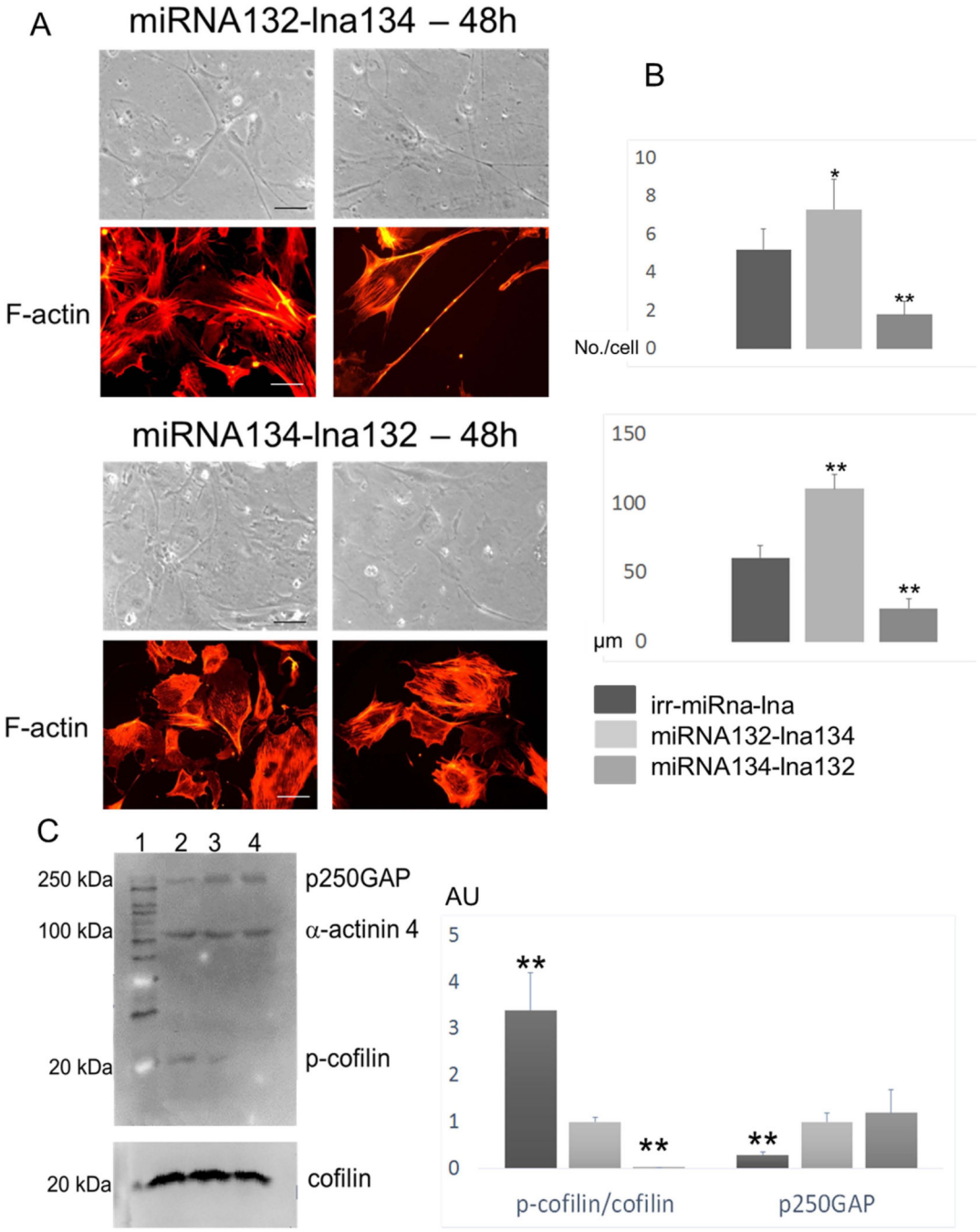

Fig 3. BDNF has opposite actions on miRNA134 and miRNA132. Double transfection mimics BDNF effects

A) Results of double transfection are shown by brightfield microscopy and F-actin. The upper four panels show the presence of numerous elongated cell processes after 48h miRNA132 overexpression coupled to miRNA134 silencing. In the lower four panels cells look rounded and depleted of cell processes after 48h miRNA134 overexpression and miRNA132 silencing. Scale bars 50µm.

B) Quantification of number (upper graph) and length (lower graph) of cell processes 48h after double transfection with controls (sense miR-159 control, miRCURY LNA™

knockdown probe) (dark-gray bars), miRNA132 overexpression coupled to miRNA134 silencing (pale-gray bars) and miRNA134 overexpression coupled to miRNA132 silencing (gray bars).

C) WB analysis of p-cofilin (upper blot, 20kDa band), and p250GAP (upper blot, 250 kDa band) demonstrates increased cofilin phosphorylation and reduced p250GAP after 48h from cell transfection inducing miRNA132 overexpression coupled to miRNA134 silencing (lane 2), as compared to transfection with control clones (lane 3). P-cofilin is no more detectable, whereas p250GAP does not show changes when miRNA134 is overexpressed and miRNA132 is silenced (lane 4). Alpha-actinin 4 (band at 100 kDa) and total cofilin (lower blot) are the loading controls. Lane 1: molecular weight marker.

The graph displays results from three experiments. Y axis: arbitrary units. Dark-gray bars: miRNA132 overexpression plus miRNA134 silencing; pale-gray bars: control clones; gray bars: miRNA134 overexpression plus miRNA132 silencing.

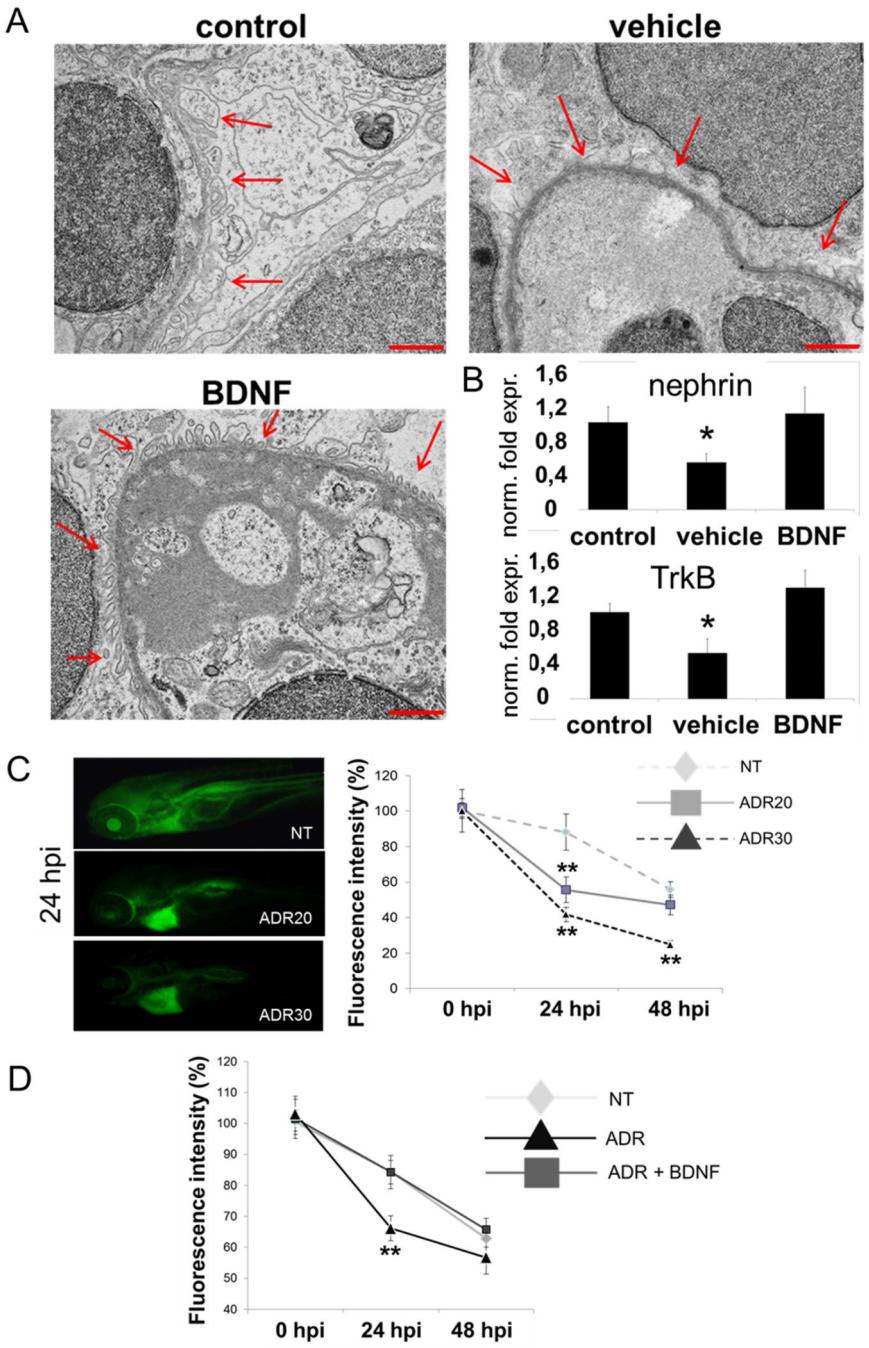

Fig 4. BDNF repairs podocyte damage in Zebrafish larvae

A) Transmission Electron Microscopy of representative glomeruli from 5 dpf larvae. In control conditions (upper left image) regularly spaced podocyte foot processes cover the basement membrane (red arrows). After vehicle treatment (upper right image) very few podocyte foot processes can barely be recognized (red arrows) and most of the basement membrane looks diffusely covered by the podocyte cytoplasm. After BDNF treatment (lower left image) podocyte foot processes look similar to the control condition (red arrows). Scale bars 1μm.

B) Real-Time RT-PCR for nephrin (upper graph) and TrkB1 (lower graph). mRNA was obtained from 5 dpf Zebrafish larvae in control conditions and after vehicle and BDNF treatment (10 animals per group). Vehicle treatment determines a significant reduction of both nephrin and TrkB mRNAs. Their expression after BDNF treatment is similar to controls. Y axis: normalized fold expression.

C) The images on the left show distribution of injected fluorescent dextran at 24 hours post-injection (hpi). As predicted, fluorescence is distributed throughout the body in a zebrafish larva in control conditions (NT). Incubation with adriamycin dose-dependently (ADR20, ADR30) decreases fluorescence at 24hpi, while accumulation due to pericardial edema can be seen in the cardiac area. The graph on the right illustrates measurements of eye fluorescence at injection (0 hpi) and after 24 and 48 hours. Measurements were taken from 30 animals per group.

D) Eye fluorescence at 24h is significantly lower in larvae receiving medium alone after adriamycin incubation. BDNF treatment restores fluorescence intensity at control levels. Measurements were taken from 30 animals per group. *$p<0.05$; **$p<0.01$.

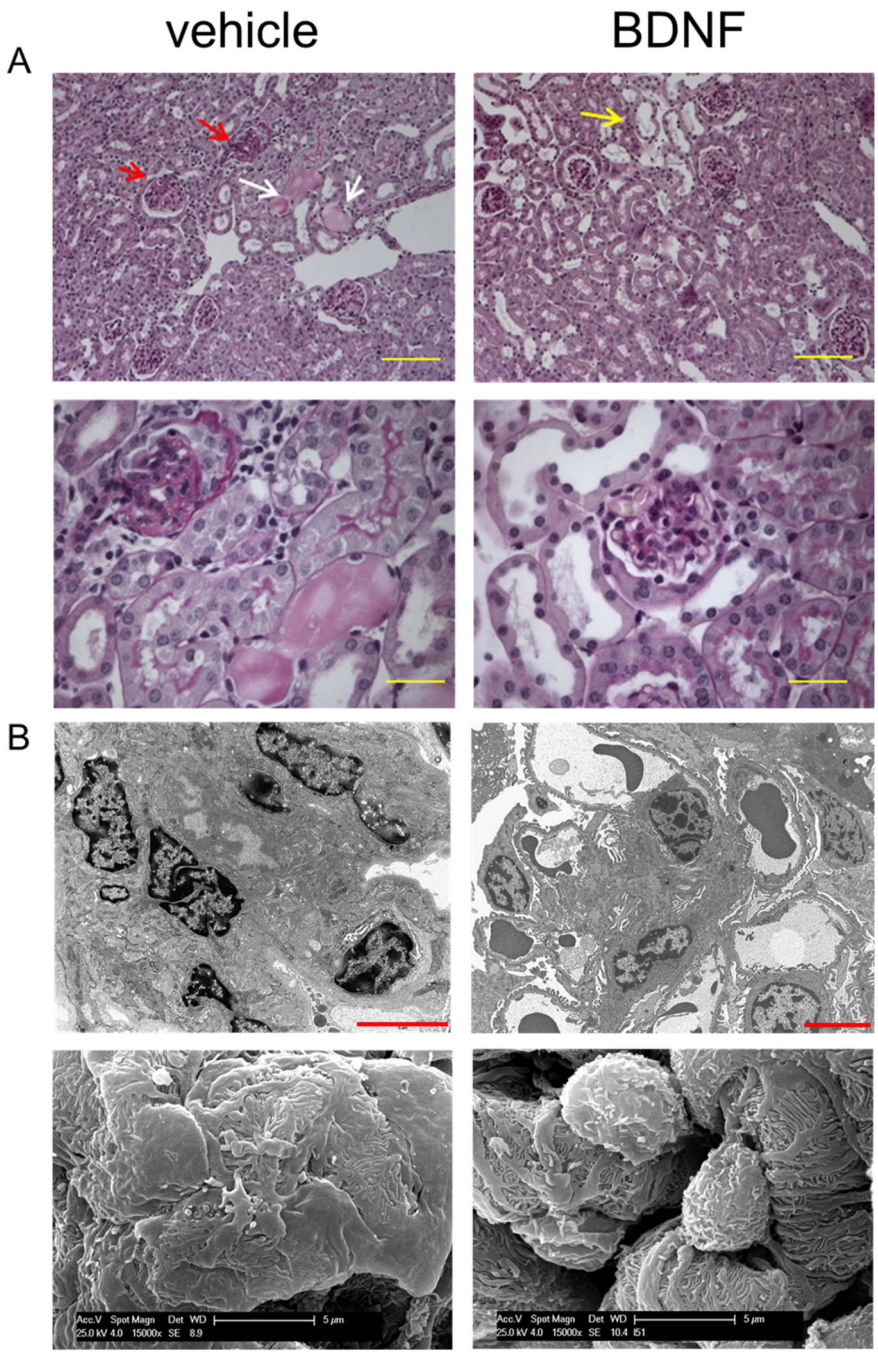

Fig 5. BDNF treatment in mouse adriamycin nephropathy

A) Representative images from vehicle-treated (left panels) and BDNF-treated mice (right panels). At low magnification (upper panels, scale bars 100μm) glomeruli with segmental sclerosis (red arrows) and dilated tubuli filled by proteinaceous material (white arrows) can be observed in the renal tissue from a vehicle treated mouse. Tubular dilation (yellow arrow) is still present after BDNF treatment, but protein casts are no more visible, and glomeruli have a normal appearance. These features can be better appreciated at higher magnification (lower panels, scale bars 50μm).

B) Transmission (upper panels) and scanning (lower panels) electron microscopy pictures show completely flattened podocyte processes from a vehicle-treated animal, and their almost normal appearance after BDNF treatment (scale bars: 5μm).

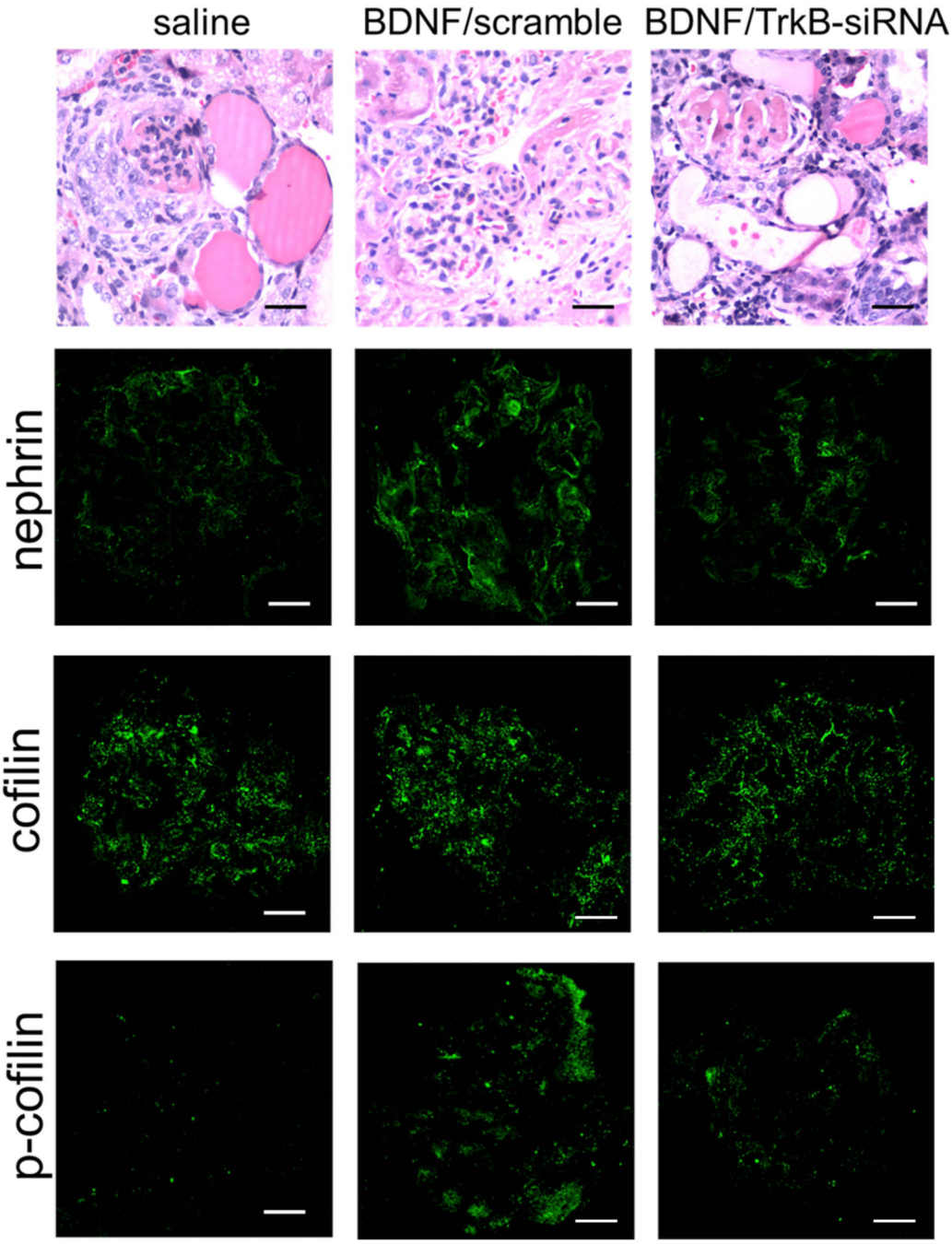

Figure 6. In vivo glomerular TrkB silencing impairs BDNF effects

Representative light microscopy (upper panels, Hematoxilin-Eosin, scale bars 50 μm) shows a damaged glomerulus surrounded by dilated tubuli filled by protein casts in a mouse treated with saline (left panel). BDNF is effective in reducing renal damage in a mouse injected with scramble siRNA (middle panel), whereas the efficacy is blunted after silencing of TrkB (right panel).

Nephrin positivity (second row) can be clearly observed in a BDNF/scramble injected animal (middle panel), whereas is barely detectable in glomeruli from a saline-treated and a BDNF/TrkB-silenced mouse.

Cofilin staining (third row) does not show major changes in all experimental conditions. Instead, P-cofilin (fourth row) is almost negative after saline (left panel) and BDNF/TrkB silencing (right panel), and is clearly positive after BDNF/scramble siRNA (middle panel). Scale bars 25 μm.